CHEMISTRY
A EUROPEAN JOURNAL

DOI: 10.1002/chem.200700003

Bridge Over Troubled Water: Resolving the Competing Photosystem II Crystal Structures

Simon Petrie, Rob Stranger,* Phillip Gatt, and Ron J. Pace[a]

Abstract: Density functional theory (DFT) calculations, at the Becke-Perdew/TZP level of theory, were used to investigate a set of $CaMn_4$-containing clusters that model the active site of the water-oxidizing complex (WOC) of photosystem II (PSII). Metal-atom positions for three representative isomeric clusters of the formula $[CaMn_4C_9N_2O_{16}H_{10}]^{+}\cdot 4H_2O$ are in good agreement with the disparate Mn_4 geometries of the three most recent X-ray crystal structures. Remarkably, interconversion between these three isomeric clusters is found to be facile, resulting from subtle changes in the coordination environment around the $CaMn_4$ centre. This result provides a clear rationalisation of the marked differences in reported crystal structures. Recent concerns have been raised regarding the opportunity for X-ray-damage-induced distortion of the metal-containing active centre during crystallographic analysis. Our calculations suggest that an even greater problem may be presented by the apparent fluxionality of the $CaMn_4$ skeleton within the active centre. Structural rearrangement may well precede crystallographic analysis, for example by the preferential "freezing-out" of one of several near-isoenergetic structures during the workup for crystallisation. This prospect, which our calculations cannot exclude, highlights the difficulties that will continue to be faced by experimentalists seeking unambiguous structural information on the WOC's active site.

Keywords: density functional calculations · metalloproteins · mixed-valent compounds · photosystem II · structure elucidation · X-ray diffraction

Introduction

The water-oxidizing complex (WOC) of photosystem II (PSII) is remarkable for its ability to promote the conversion of water to molecular oxygen. It is remarkable also for its resistance to unambiguous characterisation by the accepted laboratory techniques for obtaining structural and mechanistic data of metalloproteins. Several recent XRD (X-ray diffraction) structure characterisations[1–5] provide divergent pictures of the arrangement of metal centres in the inner $CaMn_4$ cluster of cyanobacterial PSII. Other somewhat complementary approaches, most recently EXAFS (extended X-ray absorption fine structure), provide metal–metal interatomic distances generally expected to be more accurate than those of the extant crystal structures, but still leave many aspects of the $CaMn_4$ cluster's overall geometry open to debate.

Details of the functional $CaMn_4$ centre in PSII currently unresolved include 1) the spatial interrelationship between the four manganese atoms, 2) the combined oxidation state of the Mn_4 core and 3) the nature and number of bridging ligands that connect the manganese atoms. In existing X-ray structures,[1–5] it is not possible to resolve small ligands (terminal or bridging oxo groups), while hydrogen atoms are an order of magnitude more demanding. Since the $H_2O \rightarrow O_2$ reaction probably involves OH and/or O intermediates, the necessity to distinguish between water, hydroxyl, and oxo groups is acute. This is an area in which computational chemistry is particularly valuable, since the identity of all ligands can be specified and rigorously assessed.

Previous computational studies, primarily using hybrid density functional theory, have been reported on tetramanganese clusters relevant to the PSII active site.[6–13] These studies have used the London XRD structure[3] (resolution of 3.5 Å) as a starting point. To our knowledge, no reported computational studies exist that treat the most recent (3.0 Å resolution) Berlin XRD structure.[5] The latter crystal structure has, however, been very recently reinterpreted in

[a] Dr. S. Petrie, Prof. R. Stranger, P. Gatt, Dr. R. J. Pace
Chemistry Department, the Faculties
Australian National University, Canberra ACT 0200 (Australia)
Fax: (+612) 6125-0760
E-mail: rob.stranger@anu.edu.au

Supporting information for this article is available on the WWW under http://www.chemeurj.org/ or from the author.

the context of an oriented EXAFS study[14] from which the results are more consistent with "Berlin" than with "London". Both of these crystal structures are probably different from the earlier (3.7 Å resolution) XRD structure from Japan.[2] The apparent differences in the inferred Mn cluster geometry and connectivity suggested by the structural groups are difficult to reconcile. Are these differences real, artefactual, or within the combined uncertainties of the resolution limits of the data?

Here, we report results from an extensive study using density functional theory (DFT) on tetramanganese cluster models of the water oxidizing site in PSII. Our calculations have involved optimisation of over 800 different structures (≈160 000 cpu hours). The calculations use the Berlin structure[5] as a starting point, but explore sufficient structural variety to encompass also the earlier London[3] and Hyogo[2] crystal structures. We focus also on an oxidation state (nominally $Mn^{III}Mn^{III}Mn^{III}Mn^{IV}$) believed to describe either the S_0 or the S_2 state of the active complex.[15–17] Manganese EXAFS data indicate that the active complex geometry is quite similar from S_0 to S_2.[15,18,19] Thus our density functional theory calculations[20,21] should be relevant to the crystal structures,[3,5] the effective S state of which is not precisely defined but is generally believed to correspond to S_1.

Results and Discussion

The model structures considered here minimise molecular complexity while retaining all essential ligands coordinated to, or in close proximity to, the Mn atoms as revealed by the crystal structures (see Figure 1). Thus the histidine residue His332, attached to Mn1, is represented by imidazole and the carboxylate groups of the residues Asp170, Glu189, Glu333, Asp342, Ala344 and Glu354 are modelled by formate, in a ligation pattern consistent with the Berlin structure.[5] Other coordination sites on Mn are assumed to be occupied by oxo or water ligands. The distribution of oxo bridges, on which the crystal structures themselves are silent, reflects the evidence from XRD[3,5] for Mn–Mn distances of the order of 2.7–2.8 Å (implying a di-μ-O bridging arrangement) and 3.0–3.4 Å (indicative of a mono-μ-O bridge). Exploration of other bridging architectures has strongly suggested to us that four monatomic bridges (i.e., O or possibly OH) are optimal to give geometric agreement between the computed Mn_4 skeleton and either of the two most recent crystal structures.[3,5] With three dangling carboxylates on Mn1, Mn2 and Mn4 (again, for consistency with the Berlin structure, and identifiable as Glu189, Ala344 and Asp170),[5] this still leaves our model complex with coordinatively unsaturated Mn atoms, and so we have included also up to seven explicit H_2O ligands to ensure that each Mn can adopt sixfold coordination if electronically predisposed to do so. Finally, incorporation of Ca^{2+} has been explored and has been found, incidentally, to have negligible impact on the core Mn_4 geometry.

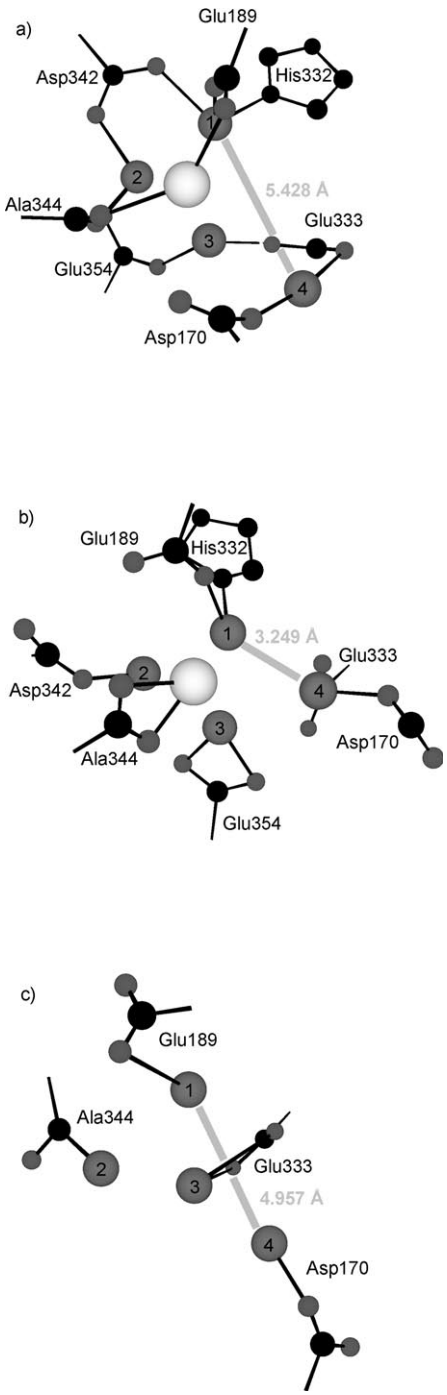

Figure 1. Comparison of a) the 3.0 Å resolution "Berlin",[5] b) the 3.5 Å resolution "London",[3] and c) the 3.7 Å resolution "Hyogo"[2] crystal structure geometries of the ligated $CaMn_4$ metal centre of PSII (the "Hyogo" structure lacks a resolved Ca atom). The chosen perspective, with the Mn1/Mn2/Mn3 triangle projected in the plane of the page, highlights the disparity in the Mn4 positions (indicated also by the marked Mn1−Mn4 distance) within the crystal structures.

The structures surveyed conform to the overall formula $[CaMn_4C_9N_2O_{16}H_{10}]^+ \cdot n\,H_2O$ ($n = 0$–7). The regularity of the formulae considered ensures that many structures are isomeric and thus their relative stabilities can be directly as-

sessed through differences in their calculated energies. An optimised structure highlighting the identification of ligands as models of individual residues is shown in Figure 2. The number of exchangeable waters in this structure—four—is close to the minimum inferred from recent ^{2}H ESEEM studies on the S_0 and S_2 states.[22]

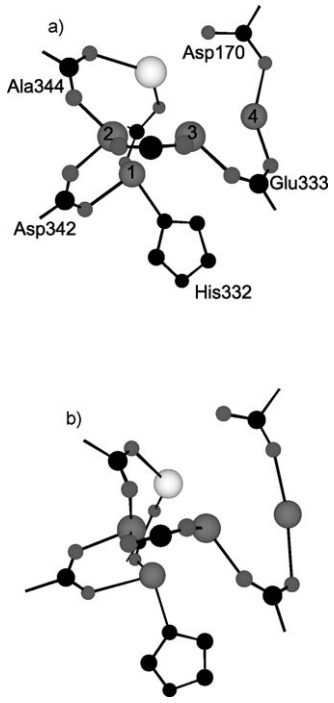

Figure 2. a) A representative optimised geometry for an isomer of $[CaMn_4C_9N_2O_{16}H_{10}]^+ \cdot 4H_2O$, hereafter identified as structure **I**, showing only those atoms seen in the 3.0 Å resolution Berlin crystal structure. Mn atoms are numbered 1 to 4 and ligands are labelled to identify the residues they model. The unlabelled formate ligands linking Mn1 and Ca (background) and Mn2 and Mn3 (foreground), respectively, are Glu189 and Glu354. b) A view of the metal core and ligation in the Berlin crystal structure.

Our calculations on hydrated $[CaMn_4C_9N_2O_{16}H_{10}]^+$ are by no means the first density functional theory investigation of a $CaMn_4$ model for the WOC. As noted in the Introduction, the groups of Siegbahn and Battista have been active in the theoretical study of PSII for the past few years. While both of those groups have employed the hybrid B3-LYP functional in their studies, we have chosen to use here a "pure" density functional (Becke–Perdew).[23,24] The Becke–Perdew functional has been found to perform very favourably in comparison to B3-LYP, in a systematic evaluation of different DFT methods applied to first-row-transition-metal-containing compounds.[26]

Other fundamental differences between the present work and previously reported computational studies relate to the $CaMn_4$ complex structures investigated by the various groups. Siegbahn and co-workers have considered a model in which the Ca atom is bridged to the central Mn pair of an effectively linear Mn-containing tetrameric complex,[25] and more recently have focussed on a structure corresponding to a $CaMn_3$-containing cubane-like skeleton featuring an externally bridged additional Mn atom.[6,9–11] The latter structure is broadly similar to that which has been reported in the works of Battista and co-workers.[12,13] The incorporation of a cubane-like feature in the structures investigated by both of these groups may well arise from the identification of this structural feature in the London XRD study.[3] Also in broad consistency with the London XRD study,[3] the most recent reported models of both the Siegbahn and Battista groups feature manganese skeletons that are held together almost exclusively by oxo and/or hydroxo bridges, augmented by only one carboxylate bridge in each instance (between Mn1 and Mn4[6] or between Mn1 and Mn3[12]). This provides a clear contrast with our own structural studies, which have focussed, for now, on complexes that feature three carboxylate bridges between Mn atoms, in keeping with the ligand environment reported from the Berlin crystal structure study.[5] Note that, since a central tenet of the present work is that the metal centre in PSII is inherently flexible as discussed below, it is not practical to attempt assessment of the various computational models against the arguably still nebulous PSII water-oxidizing complex structure.

Two key trends emerge from our calculations. First, there is a marked preference for antiferromagnetic coupling between adjacent Mn atoms, with adoption of high-spin, rather than low-spin, Mn^{III}. The high-spin Mn^{III} atoms in each structure are readily identified from the elongation of axial bonds to coordinated water and/or carboxylate ligands as a result of Jahn–Teller distortions. The relative orientations of these Jahn–Teller axes differ between structures **I**, **II** and **III** due to differences in the ligand bridging architecture. Second, during several optimisations on various structures (for which starting geometries were customarily obtained by removal of a weakly bound H_2O ligand from a previously optimised structure), spontaneous changes in the bridging between metals and/or migration of protons from water ligands to μ_2-O bridges were observed. The latter observation, of significant structural shifts driven by removal of weakly-bound ligands, suggests that the tetramanganese complex in PSII possesses an unusually high degree of structural flexibility, and thus we might expect that different $CaMn_4$ core geometries could be preferentially "frozen out" under different crystallisation conditions. Accordingly, it is not altogether surprising that the most resolved crystal structures may be at variance with each other. Two structural modifications, highlighted below, are particularly relevant to interpretation of the crystal-structure differences.

The comparison between our $[CaMn_4C_9N_2O_{16}H_{10}]^+ \cdot (H_2O)_4$ isomer **I** and the Berlin crystal structure highlights the very good agreement between theory and experiment (see Figure 2). Because the positional uncertainty of Mn4 is greatest in the Berlin structure, the latter may be a mixture of isomers **I** and **II** (Figures 3 and 4), which differ in the bridging orientation of Mn4 to Mn3. Particularly in calculations on models from which the Ca^{2+} ion is omitted, interconversion between structures of types **I** and **II** is found to

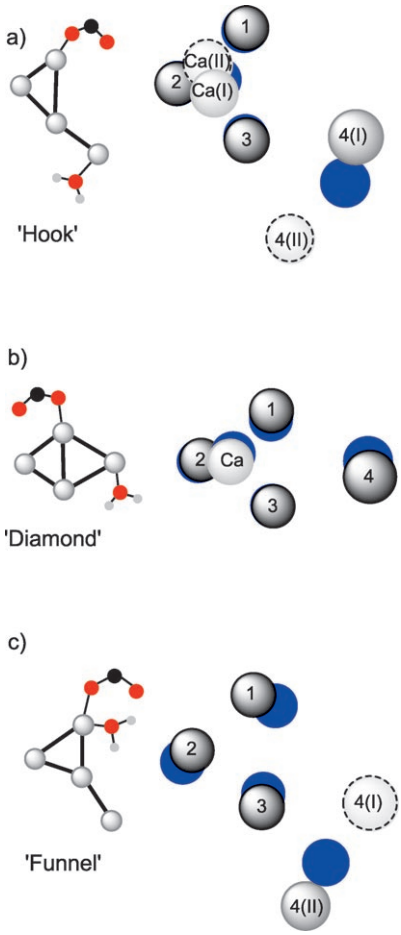

Figure 3. a) Comparison of metal-atom positions for two isomers of $[CaMn_4C_9N_2O_{16}H_{10}]^+ \cdot 4H_2O$, structures **I** (the "hook") and **II** (the "funnel"), shown as solid spheres in perspective view, with the 3.0 Å resolution Berlin crystal structure positions (shown as blue circles) for these metal atoms. Metal-atom positions for structures **I** and **II** differ significantly only for Mn4 (and to a lesser extent for Ca), resulting from the presence (in **II**) of a H_2O ligand on Mn1 which is interposed between Mn1 and Mn4 and which thus results in a much larger Mn1–Mn4 distance than seen in **I**. The crystal-structure positions for both Ca and Mn4 are intermediate between the **I** and **II** positions, but closer to **I**. b) Comparison of metal-atom and bridging oxo positions for a third isomeric structure **III** (the "diamond") with the 3.5 Å resolution London crystal structure. c) Comparison of Mn atom positions for structures **I** and **II** with the 3.7 Å resolution Hyogo crystal structure. It appears that the Hyogo structure is consistent with a significantly greater degree of H_2O-ligand coordination to Mn1 than is the case for the Berlin structure. The small inset structural figures highlight diagrammatically the key ligand-coordination differences between the theoretical structures (see text).

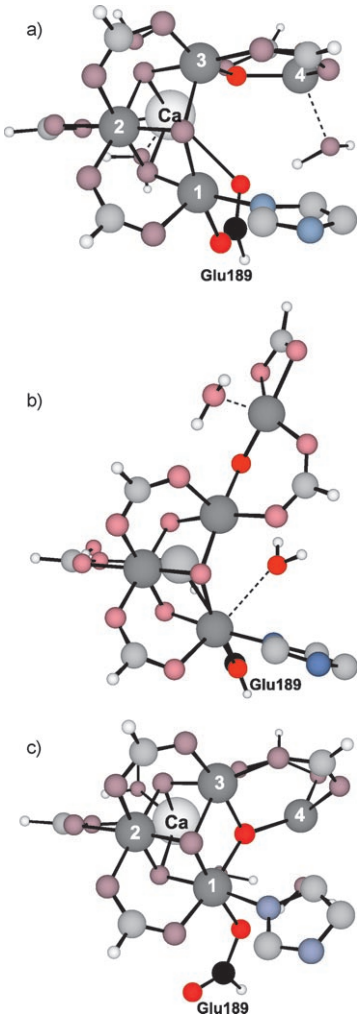

Figure 4. a) Optimised geometry of the $[CaMn_4C_9N_2O_{16}H_{10}]^+ \cdot 4H_2O$ isomer **I**, which exhibits a close similarity to the $CaMn_4$ core of the Berlin crystal structure. b) Optimised geometry of isomer **II**, which resembles the Mn_4 architecture of the Hyogo crystal structure. c) Optimised geometry of isomer **III**, which resembles the $CaMn_4$ core of the London crystal structure. For clarity, imidazole-borne H atoms on all structures have been hidden. Interconversion from **III** to **I** is effected by rotation of the highlighted carboxylate group, which coordinates to calcium in **I** (and in the Berlin structure) but not in **III** (nor in the London structure). Structure **II** also has highlighted the Mn1-coordinated H_2O ligand that is associated with the extension of the Mn1–Mn4 distance in this structure, compared with that in **I**. Also highlighted in the three structures is the oxo bridge between Mn3 and Mn4: in the upper two structures, this O atom is well out of bonding range from Mn1, while in the lowest structure the formation of a μ_3-O bridge connecting Mn1, Mn3 and Mn4 is apparent. Formation of this μ_3-O bridge is arguably the key process in converting the Berlin crystal structure's metal core into that of the London structure.

be facile and dependent on the ligation of Mn1, with structure **II** featuring a water ligand occupying a coordination site on Mn1 which is vacant in **I**. Inclusion of Ca^{2+} has a stabilizing influence on structure **II** in the sense that retention of this geometry is no longer fully dependent on hydration at Mn1, but structure **I** (with Ca^{2+} included) appears to retain the ability to "unfold" to **II** when the Mn1 site is hydrated. The fully-dehydrated **II** form of $[CaMn_4C_9N_2O_{16}H_{10}]^+$ is 20.2 kJ mol^{-1} higher in energy than the corresponding structure **I** according to our calculations, while the sequential addition of five H_2O ligands to each structure results in a consistent stabilisation of **II** relative to **I**, such that penta-hydrated **II** lies 8.6 kJ mol^{-1} *below* the corresponding **I** form. The sensitivity of the relative energy between the two structural types, with **II** favoured over **I** at higher hydration levels, supports our contention that the Hyogo and London crystal structures may well differ in

their hydration environment. In any event, our calculations across a range of hydration levels strongly suggests that the equilibrium between these **I** and **II** geometries is highly sensitive to chemical influences beyond the immediate ligation environment provided by the proximate peptide residues.

Structure **II** has the classic "funnel" motif, which was the earliest suggested form of the Mn cluster and which appears to dominate the 2003 Hyogo crystal structure (see Figure 3). A difference in the degree of hydration at Mn1 for the Berlin and Hyogo crystal structures could reflect different crystallisation conditions in the two studies.[27,28] Note that agreement with our calculated metal atom positions, particularly for the "central triangle" of Mn1, Mn2 and Mn3, is considerably better for the higher resolution Berlin structure than for the earlier Hyogo structure.

The key distinction between the Berlin and London metal cores is that the London structure features a second μ_3-oxo bridge, which is precluded in the Berlin structure by the much greater Mn1−Mn4 distance. Theoretical Mn_4- and $CaMn_4$-containing structures conforming quite closely to the London metal-core geometry can be optimised fairly straightforwardly. As an example, Figure 4 compares isomers **I** and **III**, which respectively closely resemble the Berlin and London crystal structures in their metal positions (c.f. Figures 2 and 3). We have found that the energetic separation of **I** and **III** is, in general, even narrower than that witnessed between **I** and **II**. Fully dehydrated **III** lies 1.4 kJ mol^{-1} below its **I** analogue. Further, while hydration benefits **I** over **III**, the preferred penta-hydrated geometry of **I** is only 8.6 kJ mol^{-1} below the corresponding **III** structure.

Does a mechanism exist by which **I** and **III** can readily interconvert? We believe that such interconversion effectively hinges on the orientation of the "Glu189" formate. When the optimised geometry of structure **III** is adjusted by a 90° rotation of the "Glu189" formate about the O−Mn axis, a spontaneous reorganisation occurs within the metal core, severing the bond from Mn1 to the oxo bridge shared by Mn3 and Mn4 to convert **III** to **I**. Interconversions of this type are also witnessed for several other structures, both including and excluding the hydrated Ca ion, and in the opposite direction also (i.e., involving the reshaping of a Berlin-like metal core into a more London-like structure). In all cases, the key features are a substantial change in the "Glu189" carboxylate's conformation and the concomitant formation or severing of a μ_3-oxo bridge linking Mn1 to Mn3 and Mn4. These results suggest that the different crystal-structure models for the PSII active centre may in fact be connected by something as facile as a conformational change in one of the dangling carboxylate ligands. Notably, site directed mutation studies on Glu189[29] yield ambiguous results. Moreover, four of the seven protein-derived ligands to the Mn cluster are located on a short, inherently flexible peptide region—the C terminus of the D1 protein. Such an organisation for a metalloprotein catalytic site is unique to our knowledge. It suggests a functional purpose, perhaps reflected in the structural lability we have identified here.

Table 1 reports the optimised metal–metal distances and angles for the isomers **I**, **II** and **III**, as well as the measured values for these properties in the various experimental structure studies. (A graphical comparison of our calculated metal-atom positions with the three most recent crystal structures is provided in Figure 3, and a more complete comparison, including also the earliest crystal structure and the recent EXAFS-derived structure, is depicted in the Supporting Information).

It should be noted that the optimised Becke–Perdew/TZP geometries (stereoviews of each isomer are included in the

Table 1. Comparison of Mn−Mn distances and angles in the Berlin, London, and Hyogo crystal structures, in the most recent EXAFS-derived model, and in the computed geometries **I**, **II** and **III**.

Parameter[a,b]	Berlin XRD[c] (2005, 3.0 Å)	London XRD[d] (2004, 3.5 Å)	Hyogo XRD[e,f] (2003, 3.7 Å)	Berlin XRD[f,g] (2001, 3.8 Å)	EXAFS[h] (2006)	**I**	**II**	**III**
r(Mn1−Mn2)	2.645	2.648	3.348	3.017	2.814	2.737	2.745	2.684
r(Mn2−Mn3)	2.703	2.669	2.692	2.968	3.260	2.746	2.748	2.705
r(Mn1−Mn3)	3.285	2.718	2.749	2.761	2.717	3.469	3.414	2.954
r(Mn3−Mn4)	3.245	3.255	2.709	2.754	2.712	3.338	3.110	3.273
r(Mn1−Mn4)	5.428	3.249	4.957	4.577	4.790	4.579	6.343	3.705
∢(Mn1-Mn2-Mn3)	75.8	61.5	52.8	54.9	52.5	78.5	76.9	66.5
∢(Mn2-Mn3-Mn4)	153.9	119.5	151.3	123.0	139.6	124.6	149.4	118.0
∢(Mn1-Mn3-Mn4)	112.5	65.2	130.5	112.2	123.9	84.5	152.9	72.8
∢(Mn1-Mn2-Mn3-Mn4)	58.6	25.1	159.4	−100.3	103.4	44.4	152.8	41.0
r(Ca−Mn1)	3.383	3.263	–	–	3.411	3.683	3.497	3.499
r(Ca−Mn2)	3.223	3.236	–	–	3.406	3.310	3.237	3.235
r(Ca−Mn3)	3.287	3.368	–	–	3.713	3.388	3.643	3.409
r(Ca−Mn4)	4.635	3.938	–	–	4.409	3.761	5.583	3.639
∢(Ca-Mn1-Mn2)	63.2	65.4	–	–	65.5	60.0	61.1	61.4
∢(Ca-Mn1-Mn2-Mn3)	−70.1	−77.7	–	–	−79.7	−69.4	−77.9	−74.9

[a] Bond lengths in Ångstroms and bond angles and dihedrals in degrees. [b] Numbering convention adopted is as shown in Figures 1–4. Mn1 is coordinated to His332 and/or Glu189, Mn2 to Ala344, Mn3 to Glu354 (for Hyogo, to Glu333), and Mn4 to Asp170. For the original 3.8 Å resolution Berlin XRD[1], Mn identity has been established through comparison of the unit cell coordinates for Mn atoms with the coordinates reported in the latest 3.0 Å study.[5] [c] Loll et al. 2005.[5] [d] Ferreira et al. 2004.[3] [e] Kamiya and Shen 2003.[2] [f] This crystal structure does not feature a resolved calcium atom associated with the Mn_4 cluster. [g] Zouni et al. 2001.[1] [h] Yano et al. 2006.[14]

Supporting Information) feature distances between directly bridged pairs of metal atoms that are typically 0.1–0.2 Å longer than the representative neighbouring metal-atom distances from the crystal structures. This trend is fully consistent with previous experience of this method and mirrors also a tendency found by Lundberg and Siegbahn[6] for the hybrid B3-LYP method to slightly exaggerate the metal–metal distances in $CaMn_4$ OEC models (OEC = oxygen-evolving complex). Greater discrepancies are evident in the distances between metal atoms that are not directly bridged: for example, the Mn1−Mn4 and Ca−Mn4 distances in most structures, but these discrepancies appear to arise from the substantial positional variability of Mn4 within the cluster. Note that, as discussed above, the Mn1−Mn4 distance of the Berlin 3.0 Å resolution XRD is intermediate between the values in structures **I** and **II** for this parameter, a property that holds also for the key Mn4 positional markers of *r*(Ca−Mn4) and ∢(Mn1-Mn3-Mn4). The consistency of these trends bolsters our argument that the Berlin structure[5] may represent, in essence, a statistical average of Mn1-hydrated and dehydrated structures within the single crystal. A very similar argument can also be made for the Hyogo structure, albeit less convincingly, since the Hyogo metal positions appear less well defined and also since calcium is not characterised in this structure. None of the isomeric structures **I**, **II** or **III** provide a clear match to the earliest crystal structure,[1] with a resolution of 3.8 Å and without a resolvable calcium atom in the central metal cluster. The 3.8 Å resolution structure has a "central triangle" of Mn1/Mn2/Mn3 that is broadly consistent with our various models, but features Mn4 in a position totally at variance with that exhibited in any of our models. This may well provide yet another illustration of the apparently highly variable positioning of Mn4 arising from ligand-influenced fluxionality, or may represent a limitation of the comparatively low resolution in this early crystal structure study.

The ligand orientation of Glu189 quite closely matches the corresponding carboxylate conformation in both our Berlin (**I**) and London (**III**) models. Further, the least well-determined metal position in either crystal structure (Mn4, with weak metal electron density in this region in both the Berlin[5] and London[3] structures) is also the most fluxional metal atom in our calculations. This contrasts sharply with the generally robust character of the tetrahedron formed from Mn1, Mn2, Mn3 and Ca, which appears resistant to distortion and which shows a reasonably consistent shape in all of the crystal structures (see Figures 1 and 2). The observed positional consistency of the Ca atom underscores our point that, of the five metal atoms in the cluster, it is Mn4 which effectively wields the greatest control on the cluster's overall shape, in response to subtle changes in the ligation of the various metal atoms.

A likely rationale, suggested by our results, for the poorly defined and variable position of Mn4 in the PSII crystal structures is that the native photosystem contains (or crystallographic workup produces) a range of "real" Mn_4-cluster geometries in which modest hydration/ligation environment variations of the type we have modelled actually occur. The extent to which this "structural scrambling" influences the EXAFS-inferred geometries is unclear, as only structurally well-defined subsets are likely to contribute significantly to the outer shell EXAFS data, while the full positional uncertainty is reflected in the XRD patterns. Note that this explanation may also account for the observation that the discrepancies between Berlin and London XRD orientations for the surrounding protein subunits appear to be greatest for those functional groups that are closest to the Mn_4 core, such as the Glu189 carboxylate (mentioned above) and the Asp170 carboxylate ligating the fluxional Mn4 atom. Finally, the much larger uncertainty in Mn4 position in the Berlin structure compared to the London structure (Mn4 electron density levels of 4.4σ and 7σ, respectively) is consistent with the change in bridging architecture that we ascribe to Mn4 in our models **I** and **III**. In "Berlin-like" **I**, Mn4 is tethered only to Mn3 by a carboxylate and a μ_2-oxo bridge capable of (and, in several of our calculations, manifesting) inversion to give a substantial lateral shift of Mn4 relative to the Mn1/Mn2/Mn3 triangle, as in the "Hyogo-like" isomer **II**; while in "London-like" **III**, the combination of carboxylate bridge to Mn3 and μ_3-oxo bridge connecting Mn1, Mn3 and Mn4 gives rise to a less readily distorted cluster geometry.

Finally, a point to note, particularly when comparing structures **I**, **II** and **III** corresponding to the most resolved XRD data,[4,5] is that the total variation in position of Mn4 is actually relative to a largely invariant μ_3-oxo-bridged Mn1/Mn2/Mn3 core. As the cluster locates within the protein matrix in either the Berlin or London crystal forms,[4,5] there is a significant offset displacement of both the Mn1/Mn2/Mn3 core and Mn4 units, to accommodate a similar overall protein confinement cavity (the D1 C-terminal carbon backbone is quite similar in both cases). Thus the Mn1/Mn2/Mn3 core essentially "pivots" about the μ_3-oxo position between the structures, reducing the lateral displacement relative to the protein matrix required for Mn4. This is a striking example of how the "internal" ligation energetics of the cluster determine its detailed shape, with the flexible peptide region locally accommodating this.

Comparison of the various crystal structures, by other researchers, has addressed the prospects for radiation damage of the active centre during the X-ray diffraction measurements.[14,30] While X-ray damage is a valid concern, our calculations indicate active-centre reconfiguration may occur at an earlier stage and by other mechanisms. In particular, a small set of such variations, focussed on the ligation environment around Mn1 essentially reproduces the Mn metal positions in the three most resolved crystal structures of PSII.

Because of the inherent and unanticipated chemical lability of the Mn_4 core in PSII, revealed by our calculations, we have focussed mainly on structural data which directly reveal metal positions and their uncertainties. The metal-atom geometries in the three most resolved PSII crystal structures all appear consistent with a total of four oxo bridges between Mn atoms, a feature shared by structures **I**, **II** and **III** presented here. We have not explored in detail

structures of the type inferred from the most recent EXAFS measurements,[14] with a total of five oxo bridges. However, our preliminary calculations on such systems indicate that at our chosen levels of oxidation and hydration, these geometries are prone to the rupture of the "additional" oxo bridge, providing a possible connection to the crystal structure geometries. It is also apparent that many opportunities exist for "bridge relocation", through protonation of an O atom, bridge rupture and subsequent deprotonation and reattachment; we have seen examples of all of these effects in our calculations to date. These trends indicate that the $CaMn_4$ core within PSII is a surprisingly flexible structure, probably subject to rearrangement under mild conditions. A further inference is that the unique C-terminus location of this labile $CaMn_4$ core is unlikely to be coincidental and reflects a requirement for matrix flexibility within the catalytic mechanism of water oxidation at the WOC. Exploration of these structural transformations within WOC-mimicking $CaMn_4$ complexes, for which DFT calculations appear the only practical tool, will be vital to reconcile diverse and often conflicting results from experimental studies on the PSII active site.

Conclusion

Our calculations on $[CaMn_4C_9N_2O_{16}H_{10}]^+ \cdot 4H_2O$ indicate that each of the three most recently reported WOC crystal structures, although featuring quite disparate $CaMn_4$ geometries, can be satisfactorily modelled as a member of a near-isoenergetic set of hydrated $[CaMn_4C_9N_2O_{16}H_{10}]^+$ isomers. Furthermore, mechanisms are apparent for the low-energy interconversion of these isomers. These mechanisms involve the ligation environment of Mn1, the manganese atom to which His332 is bound, and have the greatest structural effect in the position of Mn4, the manganese to which Asp170 is coordinated.

The hypothesis that interconversion is facile between isomers resembling respectively the "Berlin", "London", and "Hyogo" crystal structures provides a rationalisation for the observation of disparate metal core geometries in the aforementioned XRD studies. Another explanation for these differences has been reported recently in the context of a detailed assessment of X-ray damage in an EXAFS study. While our results do not in any way discount the risk of X-ray damage during PSII crystal-structure studies, they do suggest an additional mechanism by which the different XRD structures may have arisen. We contend that this additional mechanism needs to be considered if the extant structural data on PSII, arising from studies on single crystals and on the native system, is to be satisfactorily interpreted.

The apparent plasticity of the $CaMn_4$ metal geometry may well be connected, in a functional sense, to the unusual flexibility of its coordinating protein environment. A majority of the residues that are directly coordinated to the metal core in the WOC are located on the C terminus of the D1 protein, which contrasts sharply with the observation that most metalloproteins feature ligation environments which confer a much greater structural rigidity to the active site. We argue that this conjunction of a flexible ligation environment and a fluxional metal core is not incidental and is furthermore highly likely to be central to the mechanism of water oxidation by the WOC.

Computational Methods

Density functional theory calculations employed the Amsterdam Density Functional (ADF) program, version ADF 2004.01,[21] developed by Baerends et al.[20,31] Calculations were run on Linux-based Pentium IV computers, or in parallel mode on the AlphaSever supercomputer housed at the ANU Supercomputer Facility and operated under the Australian Partnership for Advanced Computing.

Geometry optimisations, in C_1 symmetry, used the gradient algorithm of Versluis and Ziegler[32] and featured convergence constraints twice as tight as the ADF default values. Electrons in orbitals up to and including 1s {C, N, O} or 2p {Mn} were treated in accordance with the frozen-core approximation. Calculations were unrestricted, adopting either the $S_{max} = {}^{15}/_{2}$ or "broken symmetry" (BS)[33] $M_S = {}^{1}/_{2}$ electronic configurations, describing respectively the fully ferromagnetic and consistently antiferromagnetic coupling patterns for a 15d-electron Mn_4 system. Functionals used in the calculations were the local density approximation (LDA) to the exchange potential,[34] the correlation potential of Vosko, Wilk and Nusair (VWN),[35] and the nonlocal corrections of Becke[24] and Perdew.[23] The (Slater type orbital) basis sets used were of triple-ζ-plus-polarisation quality (TZP).

Acknowledgements

R.S. and R.J.P. gratefully acknowledge financial assistance from the Australian Research Council. The authors also acknowledge the generous provision of supercomputer time on the platforms of the Australian Partnership for Advanced Computing, operating through the Australian National University Supercomputer Facility.

[1] A. Zouni, H.-T. Witt, J. Kern, P. Fromme, N. Krauss, W. Saenger, P. Orth, *Nature* **2001**, *409*, 739.
[2] N. Kamiya, J.-R. Shen, *Proc. Natl. Acad. Sci. USA* **2003**, *100*, 98.
[3] K. N. Ferreira, T. M. Iverson, K. Maghlaoui, J. Barber, S. Iwata, *Science* **2004**, *303*, 1831.
[4] J. Biesiadka, B. Loll, J. Kern, K.-D. Irrgang, A. Zouni, *Phys. Chem. Chem. Phys.* **2004**, *6*, 4733.
[5] B. Loll, J. Kern, W. Saenger, A. Zouni, J. Biesiadka, *Nature* **2005**, *438*, 1040.
[6] M. Lundberg, P. E. M. Siegbahn, *Phys. Chem. Chem. Phys.* **2004**, *6*, 4772.
[7] H. Isobe, M. Shoji, K. Koizumi, Y. Kitagawa, S. Yamanaka, S. Kuramitsu, K. Yamaguchi, *Polyhedron* **2005**, *24*, 2767.
[8] J. P. McEvoy, J. A. Gascon, V. S. Batista, G. W. Brudvig, *Photochem. Photobiol. Sci.* **2005**, *4*, 940.
[9] P. E. M. Siegbahn, M. Lundberg, *Photochem. Photobiol. Sci.* **2005**, *4*, 1035.
[10] P. E. M. Siegbahn, M. R. A. Blomberg, *Philos. Trans. R. Soc. London Ser. A* **2005**, *363*, 847.
[11] P. E. M. Siegbahn, M. Lundberg, *J. Inorg. Biochem.* **2006**, *100*, 1035.
[12] E. M. Sproviero, J. A. Gascon, J. P. McEvoy, G. W. Brudvig, V. S. Batista, *J. Inorg. Biochem.* **2006**, *100*, 786.
[13] E. M. Sproviero, J. A. Gascon, J. P. McEvoy, G. W. Brudvig, V. S. Batista, *J. Chem. Theory Comput.* **2006**, *2*, 1119.

[14] J. Yano, J. Kern, K. Sauer, M. J. Latimer, Y. Pushkar, J. Biesiadka, B. Loll, W. Saenger, J. Messinger, A. Zouni, V. K. Yachandra, *Science* **2006**, *314*, 821.
[15] H. Dau, L. Iuzzolino, J. Dittmer, *Biochim. Biophys. Acta* **2001**, *1503*, 24.
[16] D. Kuzek, R. J. Pace, *Biochim. Biophys. Acta* **2001**, *1503*, 123.
[17] P. Glatzel, U. Bergmann, J. Yano, H. Visser, J. H. Robblee, W. Gu, F. M. F. de Groot, G. Christou, V. L. Pecoraro, S. P. Cramer, V. K. Yachandra, *J. Am. Chem. Soc*, **2004**, *126*, 9946.
[18] W. Liang, T. A. Roelofs, R. M. Cinco, A. Rompel, M. J. Latimer, W. O. Yu, K. Sauer, M. P. Klein, V. K. Yachandra, *J. Am. Chem. Soc.* **2000**, *122*, 3399.
[19] M. Haumann, C. Müller, P. Liebisch, L. Iuzzolino, J. Dittmer, M. Grabolle, T. Neisius, W. Meyer-Klaucke, H. Dau, *Biochemistry* **2005**, *44*, 1894.
[20] G. te Velde, F. M. Bickelhaupt, E. J. Baerends, C. F. Guerra, S. J. A. van Gisbergen, J. G. Snijders, T. Ziegler, *J. Comput. Chem.* **2001**, *22*, 931.
[21] E. J. Baerends, J. Autsbach, A. Bérces, C. Bo, P. M. Boerrigter, L. Cavallo, D. P. Chong, L. Deng, R. M. Dickson, D. E. Ellis, L. Fan, T. H. Fischer, C. Fonseca Guerra, S. J. A. van Gisbergen, J. A. Groeneveld, O. V. Gritsenko, M. Gruning, F. E. Harris, P. van den Hoek, H. Jacobsen, G. van Kessel, F. Kootstra, E. van Lenthe, D. A. McCormack, V. P. Osinga, S. Patchkovskii, P. H. T. Philipsen, D. Post, C. Pye, W. Ravenek, P. Ros, P. R. T. Schipper, G. Schreckenbach, J. G. Snijders, M. Sola, M. Swart, D. Swerhone, G. te Velde, P. Vernooijs, L. Versluis, O. Visser, E. van Wezenbeek, G. Wiesenekker, S. K. Wolff, T. K. Woo, T. Ziegler, Amsterdam Density Functional v.2004.01, S. C. M., Theoretical Chemistry, Vrije Universiteit, Amsterdam, the Netherlands, http://www.scm.com, **2004**.
[22] K. A. Åhrling, M. C. W. Evans, J. H. A. Nugent, R. J. Ball, R. J. Pace, *Biochemistry* **2006**, *45*, 7069.
[23] J. P. Perdew, *Phys. Rev. B* **1986**, *33*, 8822.
[24] A. D. Becke, *Phys. Rev. A* **1988**, *38*, 3098.
[25] P. E. M. Siegbahn, *Q. Rev. Biophys.* **2003**, *36*, 91.
[26] F. Furche, J. P. Perdew, *J. Chem. Phys.* **2006**, *124*, 044103.
[27] J.-R. Shen, N. Kamiya, *Biochemistry* **2000**, *39*, 14739.
[28] J. Kern, B. Loll, C. Lüneberg, D. DiFiore, J. Biesiadka, K.-D. Irrgang, A. Zouni, *Biochim. Biophys. Acta* **2005**, *1706*, 147.
[29] R. J. Debus, *Biochim. Biophys. Acta* **2001**, *1503*, 164.
[30] J. Yano, J. Kern, K.-D. Irrgang, M. J. Latimer, U. Bergmann, P. Glatzel, Y. Pushkar, J. Biesiadka, B. Loll, K. Sauer, J. Messinger, A. Zouni, V. K. Yachandra, *Proc. Natl. Acad. Sci. USA* **2005**, *102*, 12047.
[31] C. F. Fonseca Guerra, J. G. Snijders, G. te Velde, E. J. Baerends, *Theor. Chem. Acc.* **1998**, *99*, 391.
[32] L. Versluis, T. Ziegler, *J. Chem. Phys.* **1988**, *88*, 322.
[33] L. Noodleman, *J. Chem. Phys.* **1981**, *74*, 5737.
[34] R. G. Parr, W. Yang, *Density Functional Theory of Atoms and Molecules*, Oxford University Press, New York, **1989**.
[35] S. H. Vosko, L. Wilk, M. Nusair, *Can. J. Phys.* **1980**, *58*, 1200.

Received: January 2, 2007
Published online: May 15, 2007

